Numerical Simulation on the Flow Field of a Vortex Flowmeter with Various Upstream Conditions

Jiann-Lin Chen, Jhih-Wei Lin
Dept. of Mechanical and Automation Engineering, I-Shou University, Kaohsiung County, Taiwan
Tel: 886-7-6577711 ext. 3223, FAX: 886-7-6578853, E-mail: james88@isu.edu.tw

Peng Chen
Zhengzhou Water Service Investment Management Co., Ltd., China
Tel:86-13323833631, E-mail: chenpeng7696178@163.com

Chin-Yi Wei
Dept. of Aeronautics and Astronautics, R.O.C. Air Force Academy, Kaohsiung, Taiwan
Tel:886-7-6268881 ext. 114, E-mail: cywei7@yahoo.com.tw

Yu-Chung Huang
Energy Management System Co., Ltd., Tainan County, Taiwan
Tel:886-6-5050207 ext. 501, Fax:886-6-5051157, E-mail: ems21tw@yahoo.com

Abstract: CFD technique has been used to simulate the flow field for a vortex flowmeter with different inflow conditions. The transient turbulent flows were simulated and the vortex shedding frequencies were obtained by FFT technique. The relation of Strouhal number versus Reynolds number with fully developed flow inlet was acquired numerically and experimentally for the standard case. The flow qualities along the piping were quantified by a specific definition. Several cases, including the asymmetric flows and unsteady sine-wave flows at the entrance, were studied and compared with the standard one. The reasons for the fundamental frequency shift caused by different inflow conditions were addressed; several conclusions and future works based on numerical simulation were suggested.

Keyword: CFD, Vortex flowmeter, Flow quality

1. Introduction

Vortex flowmeters[1-2] are increasingly used in various industries because of its high accuracy, large rangeability, linearity, low cost of investment and maintenance. This kind of flowmeter, however, has poor anti-noise disturbance ability to the pipe vibrations and fluid turbulence in practical applications. Therefore, it is sensitive to installation effects which influence the measurement accuracy. ISO 5167-1 provides certain requirements to assure accurate flow rate measurements downstream of flow disturbances due to valves, diverters, elbows, and converging pipes etc.[3]. Nevertheless, many flowmeters were installed at inadequate locations because of spatial limitation or other considerations[4-5]. In 2008, the Energy Management System Co., Ltd. (EMS Company) employed its own equipments in the laboratory, which had been approved by international standard ISO 17025[6], to evaluate the measuring accuracy of various flowmeters due to complex configurations of pipelines. It was found the measurement error from a specific vortex-type flowmeter for a 75mm piping could be estimated as high as 95%. Obviously, it indicates that the measurement accuracy of vortex flowmeters is relatively more vulnerable to incoming flow quality than other types of flowmeters. Therefore, understanding the inflow mechanism on inaccurate measurement is helpful to set new policies for installations with the limited spatial requirements. However, defining universal criteria to quantify installation effects is difficult because of meter-dependent measuring principles, which implies myriad experiments should be performed.

Experiments for studying installation effects were proceeded consecutively in the past decade[7-8]. Moreover, the experimental studies of vortex generator were placed on mostly uniform flow field in the wind tunnel to conduct, but in practical situation, most of the upstream flow fields are three-dimensional. Miau[9] investigated the uncertainty analysis about the vortex flowmeter measurement, and found that the flowmeter's accuracy was greatly affected by upstream flow conditions due to the non-linear relationship between the Reynolds number and Strouhal number for the three-dimensional non-uniform flow field. Besides, behind a tapered circular cylinder, two to three constant-frequency vortex cells of the shedding vortices along the spanwise direction have been observed in Hsiao and Chiang's experiment[10].

In decades, the applications of Computational Fluid Dynamics technique(CFD) in various industries have become more popular due to the rapid progress in computer technology including software and hardware[11-12]. CFD is not only for predicting flow fields of engineering design features, but also for applying to support experimental prediction and validation of the process. Patanker successfully developed the famous SIMPLE algorithm for solving the incompressible flow[13], which has been adopted in the present study[14]. Once the CFD code has been validated, the parameters can be set up to simulate the similar flow field in efficient approaches. In this paper, we describe the CFD technique for solving the flow field of the piping of a vortex flowmeter with different inflow conditions. Several cases, including the fully developed flow, asymmetric flow and unsteady sine-wave flow at the entrance of the piping, have been studied and compared.

2. Theoretical Approaches

To simplify the present simulation, we focus on the transient incompressible turbulent cold flow without heat generation. Besides, no-slip boundary condition for the walls is adopted.

2.1 The Governing Equations

The general transport equation in conservation form for mass and momentums in the 3D Cartesian coordinate system is as follows:

$$\frac{\partial(\rho\phi)}{\partial t}+\frac{\partial(\rho\phi u)}{\partial x}+\frac{\partial(\rho\phi v)}{\partial y}+\frac{\partial(\rho\phi w)}{\partial z}=\frac{\partial}{\partial x}\left(\Gamma\frac{\partial\phi}{\partial x}\right)+\frac{\partial}{\partial y}\left(\Gamma\frac{\partial\phi}{\partial y}\right)+\frac{\partial}{\partial z}\left(\Gamma\frac{\partial\phi}{\partial z}\right)+S \qquad (1)$$

where S is the source term, including the pressure gradient. The first term indicates the transient structure of this problem. The symbol ϕ represents 1 for continuity equation, u (velocity in x direction) in x momentum, v (velocity in y direction) in y momentum, or w (velocity in z direction) in z momentum. Γ indicates the diffusion coefficient. Since the fluid explored in this paper is water, the density is constant in the present flow field. Equation (1) can be expressed in generalized coordinates vie the finite volume method for simulation[11]. Moreover, Large Eddy Simulation(LES), one of the most effective computational tools, was selected to study the present turbulent flow field[15].

To explore the impact of inflow conditions in this study, three types of inlet, a fully developed flow, asymmetric flow and unsteady sine-wave flow, were applied. These three inlet conditions having the same flow rate complement each other, for each describes a different aspect of inflow condition. The fully developed turbulent flow, as expressed in the empirical formula of Eq. (2), is chosen to simulate the flow condition in a sufficiently long pipe.

$$V = V_c\left[1 - \frac{r}{R}\right]^{1/n} \tag{2}$$

where n is the profile index according to the flow Reynolds number; V_c is the velocity at central location in pipe; r is the radial distance; R is the pipe diameter. Meanwhile, to simulate distorted flow caused by upstream piping configuration, Eq. (3) is used to express an asymmetry flow inlet as

$$V = V_c + V_c\left[\frac{r}{R}\right] \tag{3}$$

Moreover, apart from disturbance due to piping configuration, disturbance from unsteady state upstream can be simulated by the following equation.

$$V = V_c + V_c\left[sin\left(\frac{r}{0.5R}\right)\right]\left[sin(\omega t)\right] \tag{4}$$

where ω indicates fluctuating frequency; t is time in the transient simulation. Equation (4) provides time-varying inflow velocity distribution and we can change the sine-wave fluctuation to explore disturbances caused by upstream flow.

2.2 Numerical Method

The finite volume method is a numerical approach for solving partial differential equations that calculates the values of the conserved variables averaged across the volume. The general transport equation of Eq. (1), therefore, can be formulated by the finite volume method and solved by CFD. It is clear that the pipe fittings upstream the flow meter will cause flow-field interference, thus affecting the flowmeter measurement accuracy. To quantify the flow field interference, this study refers to Miau's paper about the evaluation method of flow quality[16]. The numerical form for the departure of the axial velocity distribution over a cross-sectional plane can be written as

$$\Delta V^* = \left[\frac{1}{A}\sum_{i=1}^{m}\left(\frac{(U_x)_i}{(U_o)_i} - 1\right)^2 \Delta A_i\right]^{\frac{1}{2}} \tag{5}$$

where A indicates the cross-sectional area for the pipe, U_x for the mean axial velocity at grid i, U_o is the mean average velocity at grid i for the fully developed flow. Here i indicates grid index in radial direction; m is the total grid number; ΔA_i is the grid area at index i. According to the definition, the term ΔV^* is used in our study to express the flow departure from the fully developed flow at some cross location. Therefore, the term ΔV^* is the evaluation of how fully developed the velocity is at certain location as compared to the fully developed flow at certain Reynolds number. The operation of vortex flow meter relies on the formation and shedding of vortices from a bluff body. For mass flow rate related to vortex frequency, we can analyze the signal generated by shedding vortex to obtain mass flow rate[17,18].

3. Numerical Simulations

3.1 Validations

The serviceable Vortex flowmeter VK150 manufactured by EMS company was adopted as the model case in our simulation. The configuration of the VK150, with 150 mm in inner diameter, can be viewed in Fig. 1. Figure 1 is the solid model constructed by the CAD software, SolidWorks 3D . For the clarity of discussion, a set of coordinates was positioned inside the tube, with X-axis referring to the axial flow direction, Y-axis referring to the spanwise direction of the vortex generator, and Z-axis referring to the transversal direction of the vortex generator. Moreover, the computational domain for the standard case was established by lengthening the flowmeter's pipe, that is, 0.5 times diameter in the front end and 1.5 times diameter in the rear end. Notice that this computational domain has also been applied to other case studies in the following simulations. For this standard case, the inlet is prescribed as the fully developed flow. Outflow boundary condition is set for zero order extrapolation of properties. The no-slip condition is used for all walls. To assure to march for this transient problem stably and accurately, several numerical techniques need to be elaborated. First, the standard $\kappa - \varepsilon$ turbulent model was used in steady state flow simulation. The converged solution was then imported to the solver as initial conditions in whole domain for the transient calculation by the LES turbulent model. Second, make sure the inner-loop iterations at each time step to be sufficient to avoid error propagation in marching. Third, the time step has to be small to resolve the time domain and acquire the fundamental frequency by the Fast Fourier Transform (FFT). Fourth, the time history of the induced lift (C_L), by integrating some portion of the vortex generator, was obtained for FFT to obtain the fundamental frequency. The comparison of numerical and experimental data for the standard case is demonstrated in Fig. 2. The experiment was conducted in the laboratory of EMS company, which had been accredited according to ISO 17025 by Taiwan Accreditation Foundation. Though these two lines, shown in Fig. 2, don't coincide with each other very well, each is nearly invariant in Strouhal number with respect to a range of Reynolds numbers. The simulated data is therefore meaningful and can be applied to practical designs in vortex flowmeters by employing a correction factor. Besides, the case, with the fully developed inlet flow, is regarded as the standard case, denoted as Case A, for comparison in the following case studies.

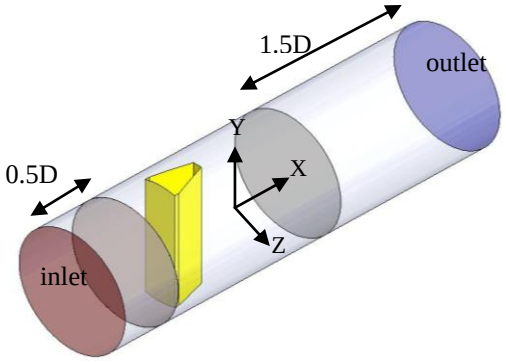

Fig. 1 Numerical model for vortex flowmeter simulation

3.2 Cases Studied

Taking the standard case as the basis, four more cases were compared to study the effect of upstream flow quality on vortex shedding. As shown in Fig. 3, the cases with asymmetric inlet flow are denoted as Case B, with Case B1 indicating the asymmetric flow along the Y-axis direction, and Case B2 indicating the asymmetric flow along the Z-axis direction. Similarly, the

cases with unsteady sine-wave inlet flow are denoted as Case C, with Case C1 indicating the sine-wave flow along the Y-axis direction, and Case C2 indicating the sine-wave flow along the Z-axis direction. According to the definition of Eq. (5), flow qualities along the axial flow direction from the inlet to the vortex generator in pipes are displayed in Fig. 4 for all study cases. Because the fully developed flow is used as the basis for comparison, the ΔV^* is zero and expressed as a dash line. Obviously, the flows from all cases depart from the fully developed flow before the vortex generator, but the flows from Case C appear like the fully developed flow. However, as the flows closer to the vicinity of the vortex generator, the flow qualities deteriorate, especially for Case B1. Generally speaking, the asymmetric flows have worse flow quality than unsteady sine-wave flows around the fore generator. Also, notice that the departures for Case C in Fig. 4 were picked up at the third second in calculation because the unsteady sine-wave inlet was variant in time.

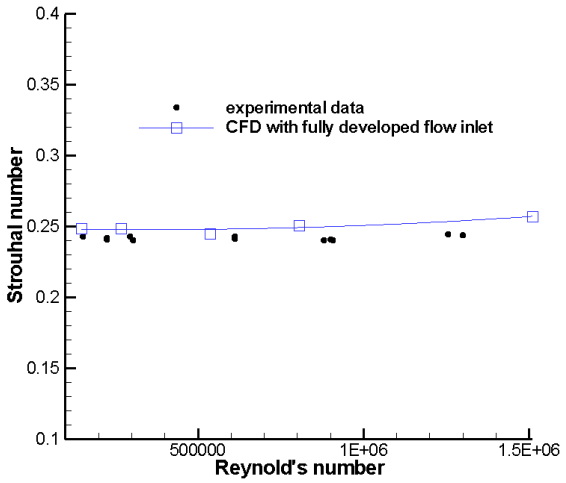

Fig. 2 Comparison of numerical and experimental data for the standard case

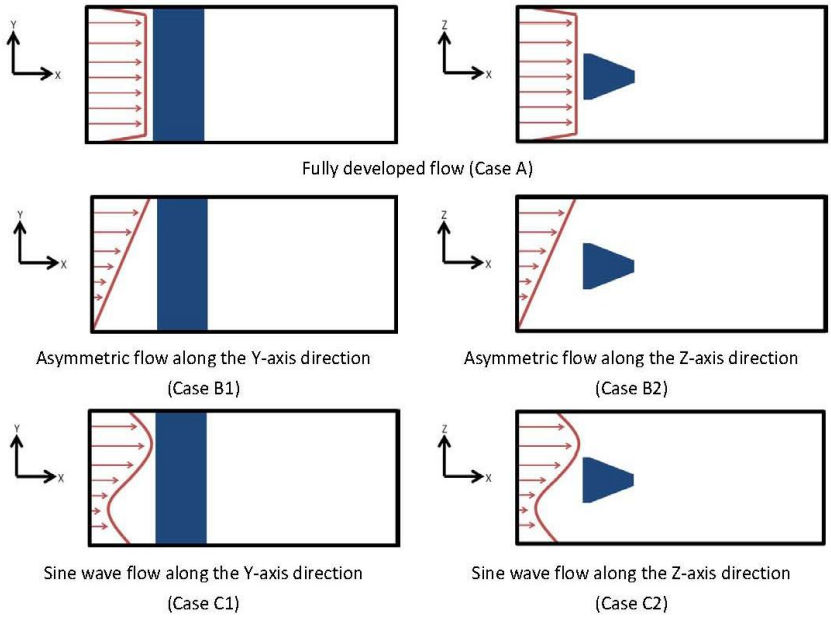

Fig. 3 Inflow conditions: fully developed flow (Case A); asymmetric flows along Y-axis and Z-axis (Case B); unsteady sine-wave flows along Y-axis and Z-axis (Case C)

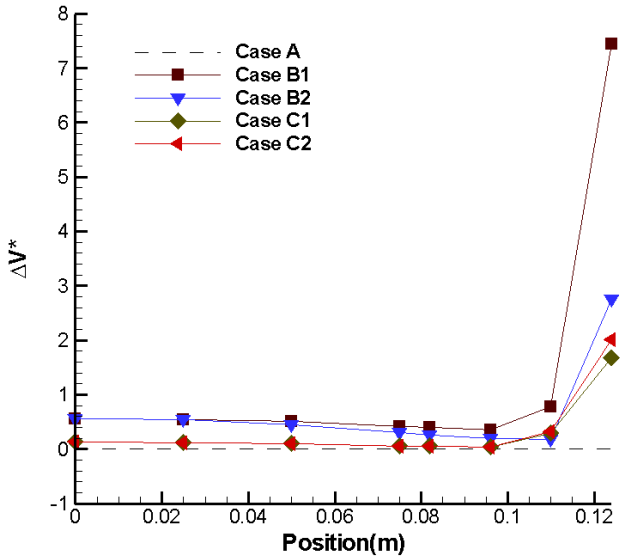

Fig. 4 Flow qualities along the axial flow direction from the inlet to generator for study cases

4. Results and Discussions

The characteristics of vortex shedding can be resolved to obtain the signals for vortex flowmeters. The pressure sensor is installed inside the pipe downstram of the vortex generator to pick up pressure fluctuation. According to Hsiao and Chiang's experiment[10], two to three constant-frequency vortex cells of the shedding vortices along the spanwise direction behind a tapered circular cylinder have been observed. Therefore, we equally separated the computational domain to 5 regions with four planes perpendicular to the Y-axis direction to see if this phenomenon exists in our simulation. The coherent structure of the vortex shedding in a cycle could be clearly observed in animated frames at the middle plane in region 3 for Case A. In fact, the plane in each region for Case A showed the similar structure of vortex shedding.

The data by performing the FFT technique is listed in table 1. The fundamental frequency in the second column was acquired by integrating the whole surface on the generator to get the total lift versus time for FFT. Similarly, the fundamental frequency for each region was calculated by integrating the surface on the generator in each region to get the lift versus time for FFT. It is shown that the fundamental frequencies are the same for all regions and the whole region. In fact, we have found that the flow structure at each plane of each region appeared similar, and it has been confirmed by visualizing their flow animations. However, we didn't find any different vortex cells as described in Hsiao and Chiang's work. A partial explanation for this may lie in the fact that our vortex generator is geometrically uniform. Besides, circular wall boundary of the pipe may enhance the coherent structure of the vortex shedding. In terms of the type with asymmetric inlet flow, the flows distorted by upstream piping configurations were simulated in Case B. The asymmetric flow along the Y-axis, Case B1, gives larger velocity difference between both ends of the vortex generator. From the flow animation, we found the coherence of the vortex shedding at the big-velocity side is obvious, and at the small-velocity side is unclear. However, the fundamental frequency appears to be the same for each region as shown in table 2, and it deviates from the fundamental frequency in Case A, nearly 20%. For Case B2, the flow pattern was substantially asymmetric at any plane in each region as viewing from the flow animation. But the vortex

shedding appeared more coherent, and the fundamental frequency closer to the one of Case A was anticipated. That is why the fundamental frequency appears the same for each region as shown in table 2. In addition, the fundamental frequency of Case B2 deviates from the one in Case A, nearly 8.3%. The final type, unsteady sine-wave inlet flow, was chosen not only for studying the effect on shedding frequency from geometrically distorted upstream, but also from unsteady upstream disturbance. Cases B have revealed that highly distorted velocity profile shifted the fundamental frequency as compared with Case A.

In Case C, the sinusoidal fluctuation enhanced the sine-wave velocity profile, this inlet flow leaded to a relatively complicated flow structure. The peak velocity took place around one side at inlet either for Case C1 or Case C2. In fact, the flow was likely to be symmetric with respect to the Y-axis direction for Case C1. However, the flow was asymmetric along the Y-axis, and it yielded velocity difference between both ends of the vortex generator. From the flow animation, we found the flow structures of the vortex shedding at planes in regions 2, 3 and 4 were coherent, while not in region 1 and 5. Interestingly, the fundamental frequencies appear different for all regions as shown in table 3. It reveals that the unsteady inlet flow complicates the flow pattern and changes the fundamental frequencies in different regions. For Case C1 in table 3, the deviations for all regions are not the same, with regions 4 and 5 having the same negative value. This low shedding frequency might result from weak flow momentums in regions 4 and 5 due to the unsteady sine-wave inlet flow. Similar results appear in Case C2 in table 3. The deviations for all regions are not the same, with regions 1 and 5 having the large negative value. It was anticipated the flow structure of Case C2 was likely to be symmetric with respect to the X-Z plane due to the inlet flow pattern. Consequently, the deviations are the same for regions 1 and 5. The unsteady sinusoidal flow, combing with the effect of space bound due to pipe wall, actually enhance the flow complexity around the generator. Notice that the fundamental frequency for the whole region is the same as the one for region 3 in every case as show in tables 2 to 4. The frequency changes along the generators take place in Case C, which has been revealed by Hsiao and Chiang's work, though we have different models. The result suggests the location of sensor installation is vital for the signal measuring process. Overall speaking, the middle plane of region 3 is the best location to install the pressure sensor for its solid occurrence of a specific fundamental frequency.

Table. 1 Fundamental frequencies of vortex shedding for the fully developed flow at inlet

Fully Developed Flow at inlet (Case A)						
	Whole region	Region				
		1	2	3	4	5
Frequency(Hz) as reference	20.98	20.98	20.98	20.98	20.98	20.98

Table. 2 Frequency deviations of vortex shedding for the asymmetric flows at inlet

Asymmetric flow along the Y-axis at inlet (Case B1)						
	Whole region	Region				
		1	2	3	4	5
Frequency(Hz)	25.17	25.17	25.17	25.17	25.17	25.17
Deviation (%)	19.99%	19.99%	19.99%	19.99%	19.99%	19.99%
Asymmetric flow along the Z-axis at inlet (Case B2)						
	Whole region	Region				
		1	2	3	4	5

Frequency(Hz)	22.73	22.73	22.73	22.73	22.73	22.73
Deviation (%)	8.33%	8.33%	8.33%	8.33%	8.33%	8.33%

Table. 3 Frequency deviations of vortex shedding for the unsteady sine-wave flows at inlet

Sine-wave flow along the Y-axis at inlet (Case C1)						
	Whole region	Region				
		1	2	3	4	5
Frequency(Hz)	25.17	25.17	25.17	25.17	19.58	19.58
Deviation (%)	19.99%	19.99%	19.99%	19.99%	-6.66%	-6.66%
Sine-wave flow along the Z-axis at inlet (Case C2)						
	Whole region	Region				
		1	2	3	4	5
Frequency(Hz)	23.43	2.79	23.43	23.43	23.43	2.78
Deviation (%)	11.66%	-86.70%	11.66%	11.66%	11.66%	-86.70%

5. Concluding Remarks

This paper presents the impact on fundamental frequency shift downstream of the vortex generator due to various inlet flow conditions in a pipe by the CFD technique. The simulated results, which have been validated by the experiment for the standard case, suggest the followings:

1. Based on the departure definition, the flow qualities, from the inlet to the front vicinity of the vortex generator, are getting worse for all study cases as compared with the standard case. The case with asymmetric flow along the spanwise direction of the generator especially has the largest departure before the generator among others. Poor flow quality upstream of the generator causes frequency deviation, but they are not related to each other linearly.

2. The frequency changes along the generator take place in the cases with unsteady sine-wave inlet flow. It implies the location of sensor installation is crucial for signal measuring processes. The middle position downstream of the vortex generator is the best location to install the pressure sensor for its solid occurrence of a specific fundamental frequency.

3. Among the many topics to be explored in future works, some important ones can be listed as follows. Uniform velocity profile with sinusoidal fluctuation is required to simulate the effect of unsteady upstream disturbance on frequency shift. The amplitude as well as the fluctuation frequency can be varied to further study their impacts on the flow phenomena. The flow-quality departure resulting from upstream conditions due to various piping configurations is also worth exploring.

References

[1] Gotthardt, B. Mass Vortex Flowmeter. *Measurements and Control*, 172, 1995, 182-184.

[2] CNS-13979. *Vortex Flow Meter*. CNS 13979, Bureau of Standards, Metrology and Inspection, Ministry of Economic Affairs, ROC, 1999.

[3] ISO-5167:2003. *Measurement of fluid flow by means of pressure differential devices inserted in circular cross-section conduits running full - Part 1: General principles and requirements*. ISO 5167-1:2003, International Organization of Standards, 2003.

[4] Takamoto, M., Utsumi, H., Watanabe, N. and Terao, Y. Installation Effects on Vortex Shedding Flowmeters. *Flow Meas Instrum*, 4, 4, 1993, 277-285.
[5] Raisutis, R. Investigation of the flow velocity profile in a metering section of an invasive ultrasonic flowmeter. *Flow Meas Instrum*, 17, 4, 2006, 201-206.
[6] ISO/IEC:17025. *General requirements for competence of test and calibration laboratories*. Geneva, Switzerland, 2005.
[7] Fletcher, S. I., Nicholson, I. G. and Smith, D. J. M. An investigation into the effects of installation on the performance of insertion flowmeters. *Flow Meas Instrum*, 11, 1, 2000, 19-39.
[8] Amadi-Echendu, J. E., Zhu, H. and Higham, E. H. Analysis of signals from vortex flowmeters. *Flow Meas Instrum*, 4, 4, 1993, 225-231.
[9] Miau, J. J., Yeh, C. F., Hu, C. C. and Chou, J. H. On measurement uncertainty of a vortex flowmeter. *Flow Meas Instrum*, 16, 6, 2005, 397-404.
[10] Hsiao, F. B. and Chiang, C. H. Experimental study of cellular shedding vortices behind a tapered circular cylinder. *Experimental Thermal and Fluid Science*, 17, 3, 1998, 179-188.
[11] Chen, J. L. *The simulation of mixed convection in a vertical chanel with ans without local blowing/suction via revised finite volume method and SIMPLER algorithm*. Naational Cheng Kung University, Tainan, 1991.
[12] Chen, C. K., Wang, L., Yang, J. T. and Chen, L. T. Experimental and computational analysis of periodic flow structure in oscillatory gas flow meters. *J Mech*, 22, 2, 2006, 137-144.
[13] Patanker, S. V. *Numerical heat transfer and fluid flow*. Hemisphere Pub. Co, New York, 1980.
[14] Jeng, Y. N. and Chen, J. L. Geometric conservation law of the finite-volume method for the SIMPLER algorithm and a proposed UPWIND scheme *Numerical Heat Transfer, Part B: Fundamentals*, 22, 2, 1992, 211-234.
[15] Lübcke, H., Schmidt, S., Rung, T. and Thiele, F. Comparison of LES and RANS in bluff-body flows. *Journal of Wind Engineering and Industrial Aerodynamics*, 89, 14-15, 2001, 1471-1485.
[16] Miau, J. J., Wu, C. W., Hu, C. C. and Chou, J. H. A study on signal quality of a vortex flowmeter downstream of two elbows out-of-plane. *Flow Meas Instrum*, 13, 3, 2002, 75-85.
[17] White, F. M. *Fluid Mechanics*. McGraw–Hill, 2003.
[18] Brigham, E. O. *The Fast Fourier Transform and Its Applications*. Prentice-Hall, Inc., Englewood Cliffs, NJ, 1988.